Journal of Ceramic Processing Research. Vol. 18, No. 5, pp. 378~384 (2017)

J O U R N A L O F
Ceramic Processing Research

Synthesis of TiO_2-polycrystalline microspheres and its microstructure at various high temperatures

Hari Sutrisno* and Sunarto

Department of Chemistry Education, Faculty of Mathematics and Natural Science, Yogyakarta State University, Campus Karangmalang, Yogyakarta 55281, Indonesia

TiO_2-polycristalline microspheres were prepared by wet chemical synthesis using titanium aquo oxo chloride ($[Ti_8O_{12}(H_2O)_{24}]Cl_8.HCl.7H_2O$) as titanium source. The morphology and structure of sample was observed using high resolution scanning electron microscopy (HR-SEM), high resolution transmission electron microscopy (HR-TEM), FT-Raman spectroscopy, FT-IR spectroscopy, X-ray diffraction (XRD) and high temperature X-ray diffraction (HT-XRD). Microstructure of TiO_2 phases were determined from HT-XRD measurement data at various temperatures from 100 °C to 1000 °C at intervals of 50 °C. The morphology of sample shows a distribution of microspheres of approximately 0.5 to 1.0 mm. Detailed measurements of sample from XRD spectra exhibit monoclinic structure (TiO_2(B) phase) of TiO_2-polycristalline microspheres. The HT-XRD results indicated that diffraction peaks of TiO_2-polycrystalline microspheres are indexed as TiO_2(B) phase from 100 to 250 °C and as anatase phase from 300 to 650 °C, while mixed crystals of anatase and rutile were observed at temperatures measurement from 700 to 800°C. Finally, pure rutile phase has formed at temperatures measurement from 850 to 1000 °C. The results of microstructure analysis show that the anatase structure could be indexed to $I4_1/amd$ (no. 141) space group with tetragonal symmetry at temperatures measurement: 600 and 750 °C, while the rutile structure could be indexed to $P4_2/mnm$ (no. 136) space group with tetragonal symmetry at 750 and 950 °C.

Key words: Titanium dioxide, TiO_2(B), Anatase, Rutile, Microsphere.

Introduction

Titanium dioxide (TiO_2) has been the subject of a great deal of research during the last decades because of its excellent optical, chemical and electrical properties. TiO_2 has a wide range of applications for the development of dye-sensitized solar cells (DSSCs) [1-3], photocatalysts for the degradation of water and air pollutants [4], self-cleaning [5], gas sensors [6], photoluminescent materials [7], photoelectrochemistry [8], super hydrophilic [9-10], light-induced amphiphilic surfaces [11] and antibacterial applications [12-13].

In fact, TiO_2 consists of eleven phases (polymorphs): anatase (tetragonal, $I4_1/amd$) [14-15], rutile (tetragonal, $P4_2/mnm$) [15-16], brookite (orthorhombic, *Pbca*) [17], TiO_2(B) (Monoclinic, $C2/m$) [18], TiO_2(H) (tetragonal, $I4/m$) [19], TiO_2(R) (orthorhombic, *Pbnm*) [20], collumbite (TiO_2-II) (orthorhombic, *Pbcn*) [21], badeleyite (TiO_2-MI) (monoclinic, $P2_1/c$) [22], TiO_2-orthorhombic (TiO_2-OI) (orthorhombic, *Pbca*) [23], fluorite (cubic, *Fm3m*) [24] and cottunite (orthorhombic, *Pnma*) [24]. All of the polymorphs contain edge- and corner-linked, octahedrally coordinated Ti cations (TiO_6). In nature, TiO_2 has three different structure types: rutile, anatase, and brookite. All of these crystalline forms of TiO_2 occur in nature as mineral, but only rutile and anatase have been able to be synthesized in pure form at low temperature. Among the TiO_2 polymorphs, anatase is the phase that contains the highest octahedral condensation. In many cases, anatase exhibits higher activity than other TiO_2 polymorphs [25-26].

Nevertheless, the material properties of TiO_2 nanoparticles are a function of the crystal structure (phase), nanoparticle size, and morphology and are strongly depend on the method of synthesis [27-29]. Numerous methods have been developed for the fabrication of one-dimensional TiO_2 nanostructures, such as self-assembling, template growth and strong alkali treatment [30-31]. These techniques mainly require high pressure, surfactant or surface capping agents. Therefore, a simple approach for a low-cost, low-temperature and controlled growth process to produce TiO_2 nanostructures is essential [32-34]. The objective of the research is to prepare TiO_2 nanoparticles by wet chemical synthesis in the absence of a surfactant or surface capping agents. The crystal structure and surface morphology of the prepared materials were studied by HRSEM, HRTEM, FT-Raman, FT-IR and XRD. The microstructure of TiO_2 phases were determined from HR-XRD measurement data at various temperature ranges from 100 °C to 1000 °C at intervals of 50 °C.

*Corresponding author:
Tel : +62 274-550836
Fax: +62 274-520326
E-mail: sutrisnohari@uny.ac.id

Experimental Procedure

Materials

Wet chemical synthesis was employed to synthesize titanium dioxide from titanium aquo-oxo chloride as titanium source. Materials used were titanium aquo-oxo chloride ($[Ti_8O_{12}(H_2O)_{24}]Cl_8 \cdot HCl \cdot 7H_2O$), silver nitrate ($AgNO_3$, Merck) and ethanol (100% C_2H_5OH, Merck).

Preparation of TiO_2-polycrystalline microspheres

In particular synthesis, 0.5 g (3.439×10^{-4} mol) of $[Ti_8O_{12}(H_2O)_{24}]Cl_8 \cdot HCl \cdot 7H_2O$ dissolved in 25 ml ethanol was added with stirring a solution containing 0.297 g (2.752×10^{-3} mol) of silver nitrate ($AgNO_3$) in 25 ml ethanol. The formation of a silver chloride (AgCl) precipitate was spontaneous. After separation of AgCl by filtration, the recovered clear solution (filtrate) was boiled to evaporation of half its volume. After filtration and drying at room temperature, a new precipitate appears was characterized by the HR-SEM, HR-TEM, FT-Raman spectroscopy, FT-IR spectroscopy and XRD. The determination of the crystal structure in the precipitate was carried out at room temperature. The microstructures of TiO_2 phases were determined from XRD measurement data at various temperature ranges from 100 °C to 1000 °C at intervals of 50 °C.

Instruments

The morphology of the precipitate was examined using HR-TEM (H9000NAR, Hitachi and HR-SEM (Jeol JSM 7600F). The FT-IR was carried out with a infra-red spectrometer FT-IR Bruker Vertex 70. FT-Raman spectra was obtained at room temperature using a FT-Raman Spectrophotometer (Bruker RFS100) equipped with a 1064 nm laser as the incident light, which allows one to focus a sample area with a diameter less than 1 mm. The XRD measurements were carried out in the reflection mode on a Siemens D5000 "PSD" model diffractometer with Cu Kα radiation (λ = 1.5406 Å). The XRD data were collected at a scanning rate of 0.02 °/s in 2θ ranging from 5 ° to 85° using standard Bragg-Brentano diffraction geometry.

Microstructure analyses of TiO_2

The techniques currently available for structure determination from powder diffraction (SDPD) data can be subdivided into two categories-"traditional" and "direct-space" approaches [35]. In this research, the ab-initio crystal structure determination of the TiO_2 phases from the sintering process at various temperatures from XRD data was performed using the two-stage method which is a "traditional" approach [36]. In the first stage, the experimental pattern is decomposed in single Bragg integrated intensities, which are then used in the second stage for solving the crystal structure by direct methods or by Patterson techniques. The whole powder pattern decomposition methods (WPPD) are used for the purpose of partition and extraction of the integrated intensities from the observed diffractograms. The WPPD is conducted using a Fullprof program (Le Bail algorithms) that is integrated with Winplotr package program to obtain the structure factor amplitudes [37]. The atomic coordinates and anisotropic parameter are generated through direct method or by Patterson techniques using ShelXS program and ShelXL integrated in Oscail-X [38].

Results and Discussion

Characterization of TiO_2 microspheres

The morphology of the precipitate was analyzed using HR-SEM. HR-SEM images of the precipitate under two magnifications are shown in Fig. 1. As can be seen from the morphologies of particles, there are a distribution of microspheres of approximately 0.5 to 1.0 mm. The crystallite size was examined using HR-TEM. Fig. 2 shows the HR-TEM images of the surface of microspheres. It is obvious from these images that the surface of microspheres are composed of TiO_2 polycrystalline with an average crystallite size of 5 nm.

The XRD was employed to further investigate the

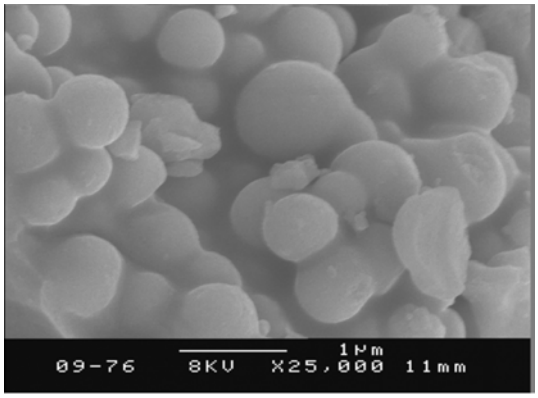

(a)

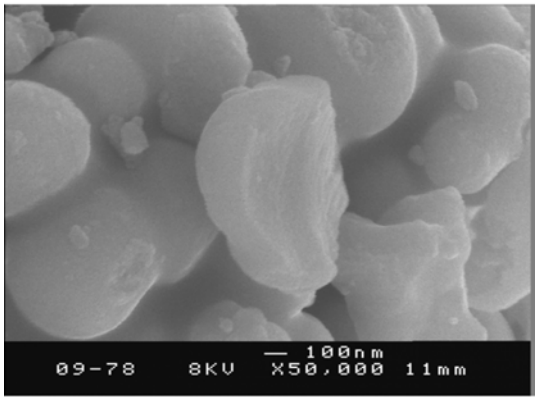

(b)

Fig. 1. Typical HR-SEM images of TiO_2 microspheres; (a) x25.000 and (b) x 50.000.

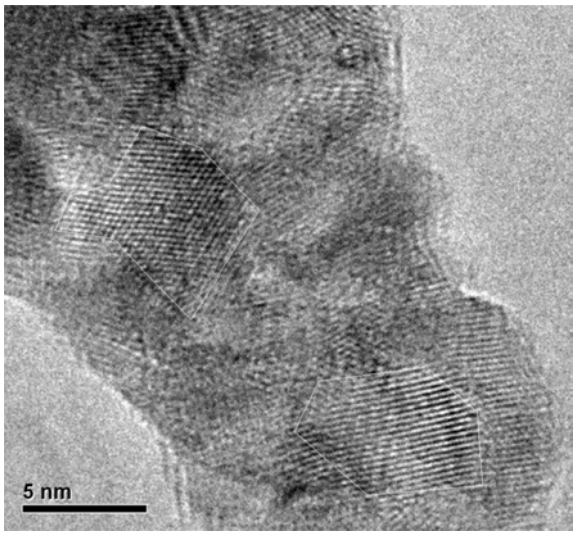

Fig. 2. HR-TEM of TiO_2-polycrystalline.

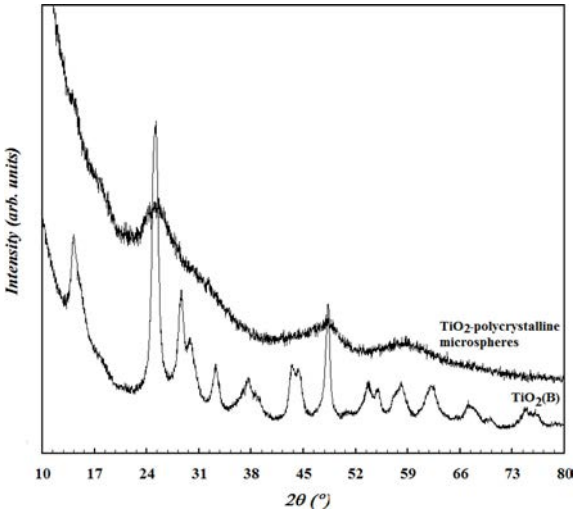

Fig. 3. XRD pattern of TiO_2-polycrystalline and TiO_2(B).

crystalline phase of the TiO_2-polycrystalline microspheres. A typical XRD pattern of the TiO_2-polycrystalline microspheres and TiO_2 (B) are shown in Fig. 3. The low and large peaks in Fig. 3(b) confirmed the TiO_2-polycrystalline microspheres were not well crystallized. The XRD patterns (Cu-Kα radiation, λ = 1.5406 Å) (Fig. 3) exhibit diffraction peaks at 2θ of 14.04, 17.80, 25.26, 30.23, 48.17 and 58.98 °, which can be readily indexed to the TiO_2 (B) phase. The peaks located at 2θ = 14.04, 17.80, 25.26, 30.23, 48.17 and 58.98 ° are indexed as the (001), (201), (110), ($\bar{4}$01), ($\bar{5}$12) and ($\bar{7}$11) planes of TiO_2(B) [39-40].

The FT-Raman spectra of TiO_2-polycrystalline microspheres was recorded between 25 and 3500 cm^{-1} in Fig. 4. The FT-Raman peaks exhibit at wavenumber of 124, 160, 197, 245, 423, 467, 495, and 632 cm^{-1}, which can be readily indexed to the characteristic bands for TiO_2(B) phase [39, 41]. The peaks located at 759, 940 and 1048 cm^{-1} are characteristic of the

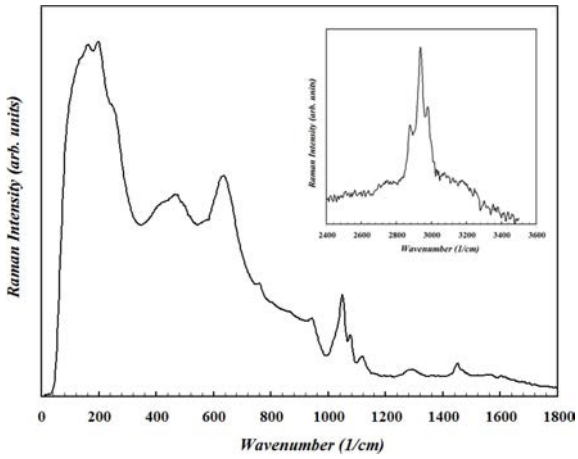

Fig. 4. FT-Raman spectrum of TiO_2-polycrystalline.

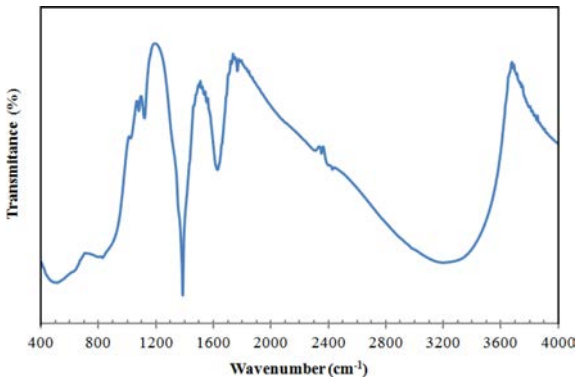

Fig. 5. FT-IR spectrum of TiO2-polycrystalline.

existence of the NO_3^- anion [42]. The peaks around 1356, 1625 and a strong stretching vibration of O-H group with the wide bands at 2900-3100 cm^{-1} are possibly be due to the stretching and bending vibration of hydroxyl groups of molecular water [43].

Fig. 5 presents the FT-IR spectra of TiO_2-polycrystalline microspheres. The peaks around 1356, 1625 and a strong stretching vibration of O-H group with the wide bands at 3000-3700 cm^{-1} (maximum around 3218 cm^{-1}) are possibly due to the stretching and bending vibration of hydroxyl groups of molecular water [44-45]. The presence of a fine and intense line at 1381 cm^{-1} and 1625 cm^{-1} reflects the existence of nitrate NO_2-symmetric and nitrat NO_2-asymmetric stretching respectively [45]. Two sharp peaks at 502 cm^{-1} and 800 cm^{-1} observed for products were attributed to vibration modes of Ti-O [42].

The relatively high intensity of the peaks associated with the hydroxyl groups and NO_3^- anion at FT-Raman (Fig. 4) and FT-IR (Fig. 5) spectra suggested that a large amount of hydroxyl groups and NO_3^- anion were located on the surface and in the layers of the TiO_2-polycrystalline microspheres.

The TiO_2 phases at various high temperatures measurement

Fig. 6 shows XRD pattern of the development of

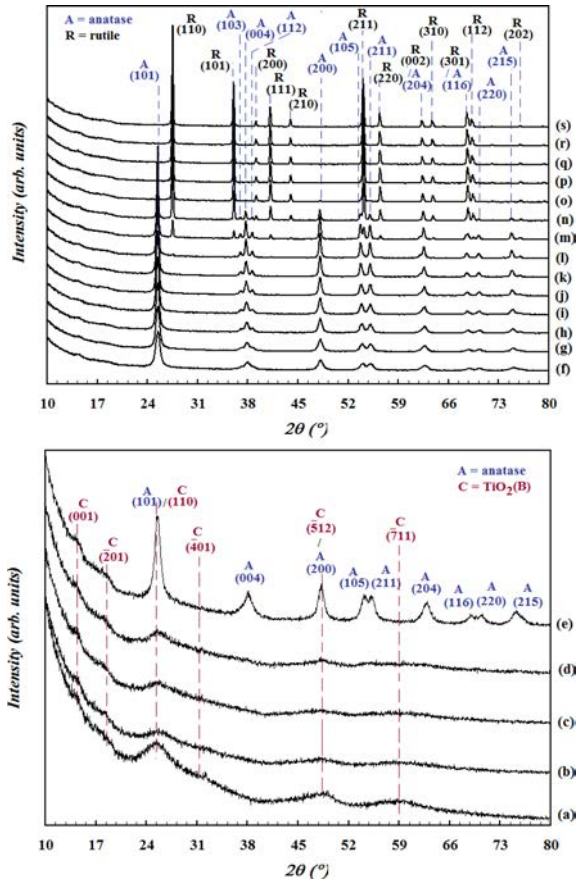

Fig. 6. HT-XRD patterns of TiO_2(B), anatase and rutile phases were recorded at temperatures measurement: (a) 100 to (s) 1000 °C at intervals of 50 °C.

structure in TiO_2-polycrystalline microspheres were recorded at 100 (a) to 1000 °C (s) with intervals of 50 °C. Diffraction peaks are indexed as those originating from monoclinic TiO_2(B) phase at temperature measurement from 100 to 250 °C. As the temperature measurement increases from 300 to 750 °C, the anatase phase becomes sharper up to 650 °C, and thereafter, rutile peaks became sharper and narrower, indicating improvement in the crystallinity of the anatase phase up to 650 °C, and thereafter rutile TiO_2 phases. After 800 °C (Fig. 6(o)) pure rutile phase has formed and the anatase phase disappears completely.

All the observed peaks could be indexed to $I4_1/amd$ space group with tetragonal symmetry for anatase or $P4_2/mnm$ space group with tetragonal symmetry for rutile. The refined parameters included Bragg intensities, the 2θ zero offset, the unit-cell parameters, the background parameters and the peak-shape parameters. The results of crystal system, cell parameters and quality of refinements from TiO_2-polycrystalline microspheres at various temperatures measurement are presented in Table 1. The X-ray diffraction pattern shows TiO_2 phase on the temperature: 100 to 250 °C is TiO_2(B), then 300 to 650 °C is dominated by anatase phase, and 700 to 800 °C is showed presenting two phases of TiO_2: anatase and rutile, then in 850 to 1000 °C is dominated by rutile phase. The main diffraction peaks at Fig. 6(a-d) are indexed as the (200), (201), (002), (400), and (402) reflections of TiO_2(B) phase. The main diffraction peaks (Fig. 6(i-l)) are indexed as the (101), (103), (004), (112), (200), (105), (211), (213), (204),

Table 1. The results of Fullprof patern matching of the XRD data of TiO_2-polycrystalline microspheres at various temperatures measurement: crystal system, TiO_2 phase, space group, lattice parameters and indicator (criteria of fit).

Temperature measurement (°C)	TiO_2 phase	Crystal system	Space group	Unit Cell (Å)		Volume (Å^3)	Quality of the refinement					
				a	b		R_p	R_{wp}	R_{exp}	2	R_B	R_F
300 (e)	Anatase	Tetragonal	$I4_1/amd$	3.79930	9.53094	137.576	3.66	4.82	5.54	0.76	0.598	0.412
350 (f)	Anatase	Tetragonal	$I4_1/amd$	3.79915	9.54366	137.749	4.42	5.90	5.70	1.07	0.613	0.455
400 (g)	Anatase	Tetragonal	$I4_1/amd$	3.79759	9.54905	137.713	4.17	5.78	5.78	1.00	0.583	0.508
450 (h)	Anatase	Tetragonal	$I4_1/amd$	3.79988	9.56176	138.063	4.26	5.92	5.80	1.04	0.583	0.431
500 (i)	Anatase	Tetragonal	$I4_1/amd$	3.79944	9.56457	138.072	4.44	6.18	5.82	1.13	0.602	0.452
550 (j)	Anatase	Tetragonal	$I4_1/amd$	3.79953	9.57033	138.162	4.31	5.95	5.79	1.06	0.603	0.494
600 (k)	Anatase	Tetragonal	$I4_1/amd$	3.80054	9.57794	138.345	4.27	6.13	5.72	1.15	0.734	0.697
650 (l)	Anatase	Tetragonal	$I4_1/amd$	3.80154	9.58481	138.517	5.28	8.43	5.58	2.28	0.445	0.559
700 (m)	Anatase	Tetragonal	$I4_1/amd$	3.80255	9.59252	138.702	4.54	6.56	5.81	1.27	0.271	0.312
	Rutile	Tetragonal	$P4_2/mnm$	4.62189	2.98189	63.699					1.210	1.330
750 (n)	Anatase	Tetragonal	$I4_1/amd$	3.80372	9.59749	138.859	4.47	6.39	5.88	1.18	0.791	0.788
	Rutile	Tetragonal	$P4_2/mnm$	4.62436	2.98324	63.796					0.685	0.965
800 (o)	Anatase	Tetragonal	$I4_1/amd$	3.80781	9.56159	138.638	5.57	7.74	6.15	1.58	1.260	1.370
	Rutile	Tetragonal	$P4_2/mnm$	4.62627	2.98506	63.888					0.765	0.720
850 (p)	Rutile	Tetragonal	$P4_2/mnm$	4.62864	2.98719	63.998	4.71	6.90	5.66	1.48	0.852	0.868
900 (q)	Rutile	Tetragonal	$P4_2/mnm$	4.63062	2.98889	64.090	4.70	6.51	5.69	1.31	0.717	0.569
950 (r)	Rutile	Tetragonal	$P4_2/mnm$	4.63060	2.98889	64.089	4.96	7.06	5.74	1.51	0.820	0.728
1000 (s)	Rutile	Tetragonal	$P4_2/mnm$	4.63489	2.99253	64.286	5.08	7.56	5.85	1.67	0.757	0.660

R_p = R-pattern, R_{wp} = R-weighted pattern, R_{exp} = R-expected , χ^2 = Goodness of fit, R_B = R-Bragg factor, R_F = R-structure factor.

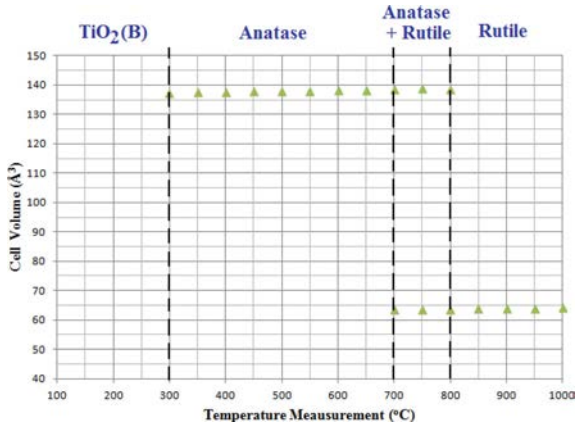

Fig. 7. Cell volume and TiO_2 phases at various temperatures measurement (TiO_2(B) < 300°C £ anatase < 700 °C ≤ anatase + rutile ≤ 800 °C < rutile ≤ 1000 °C).

(116), (220), (215) and (301) reflections of crystalline anatase phase, corresponding to those shown in the ICDD card No. 01-075-2550. The exhibited peaks (Fig. 6(p-s)) correspond to the (110), (101), (200), (111), (210), (211), (220), (002), (310), (301), (112), (111) , (202) and (212) of a tetragonal rutile structure of TiO_2, which is identified using the standard data (COD card No. 9004141). Fig. 7 shows the relationship between cell volume and type of TiO_2 phase at various temperatures measurement.

Microstructure of TiO_2 phase at 600, 750 and 950 °C

The microstructural analysis are performed on the solid at temperatures measurement: 600, 750 and 950 °C. The TiO_2-polycrystalline was measured by HTXRD at temperatures measurement of 600 °C form of TiO_2 with anatase phase, while mixed anatase and rutile phases have formed at 750 °C, and pure rutile phase is identified at 950 °C. The whole powder pattern decomposition (Le Bail algorithm) is conducted using Fullprof program that is integrated with Winplotr package program to obtain the structure factor amplitudes. The Fullprof pattern matching of 600 and 750 °C could be indexed to $I4_1/amd$ (no. 141) space group with tetragonal symmetry for anatase (Fig. 8(a) and Fig. 8(b)), while at 750 and 950 °C could be indexed to $P4_2/mnm$ (no. 136) space group with tetragonal symmetry for rutile. The refined cell parameters of anatase at 600 °C are found to be $a = b = 3.8005(20)$ Å and $c = 9.5779(20)$ Å and the unit cell volume is found to be 138.34(11) Å^3, while the cell parameters of anatase at 750°C are found to be $a = b = 3.8037(20)$ Å and $c = 9.5976(20)$ Å. These values are found to be comparable to those in Weirich et al. [14].

The refined cell parameters of rutile at 750 °C are obtained to be $a = b = 4.6241(20)$ Å and c = 2.9830(20) Å, while the cell parameters of rutile at 950°C are found to be $a = b = 4.6306(20)$ Å and $c = 2.9889(20)$ Å. These values are found in accordance with the results of the Swope et al. [16].

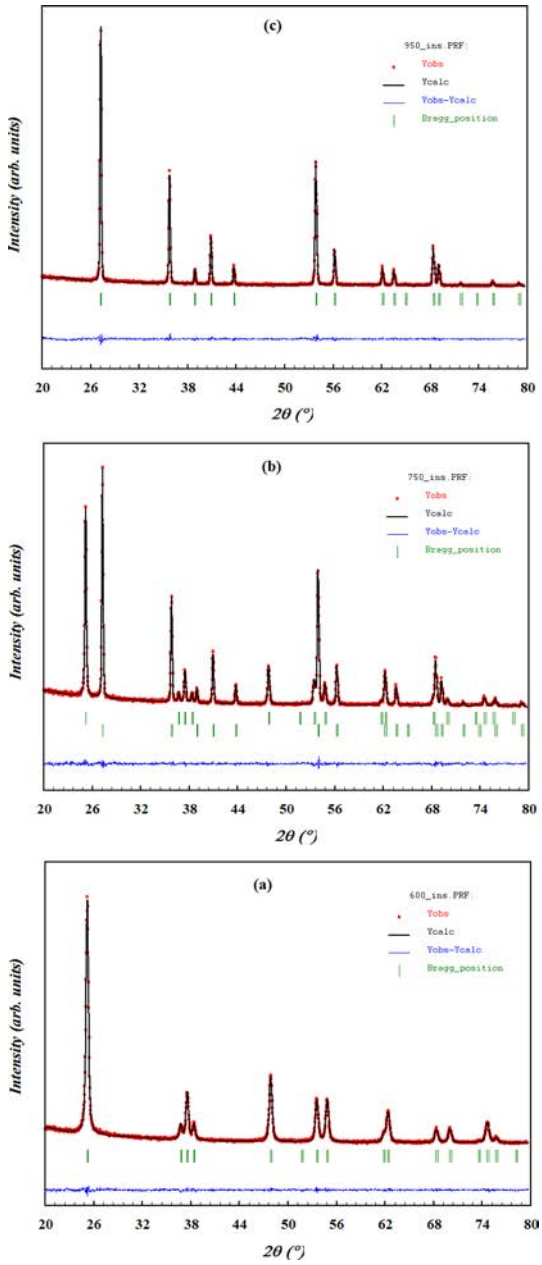

Fig. 8. Plot output showing the Fullprof pattern matching (Le Bail algorithm) to the whole powder pattern decomposition from (a) anatase (650 °C), (b) mixed: anatase and rutile (750 °C), (c) rutile (950 °C). The observed data are indicated by dot (·) and the calculated pattern is the continuous line overlying them. The short vertical lines below the pattern mark the positions of all the Bragg reflections, and the lower curve is the difference between the observed and calculated patterns plotted on the same scale.

Allowing the variation of different parameters such as cell parameters scale factors, position parameters and anisotropic thermal parameters carried out the refinement using ShelXS program and ShelXL integrated in Oscail-X. The position of the Ti and O atoms, cell parameters scale and anisotropic thermal parameters are given in Table 2.

Table 2. Basic crystallographic data for anatase and rutile phases obtained from TiO_2-polycristalline microspheres at temperatures measurement: 600, 750 and 950ºC.

Temperatures measurement	Crystal Data						
600ºC	Phase	Formula	System	Space Group	Unit Cell (Å^3)	Cell Volume (Å^3)	Density, calc. (g/cm^3)
	Anatase	TiO_2	Tetragonal	$I4_1/amd$ (no. 141)	a = 3.8005(20); c = 9.5779(20)	138.34(11)	3.835
	Atomic Coordinates						
	Atom	Position	Occupancy	x	y	z	
	Ti	4b	1	0.00000	0.00000	0.50000	
	O	8e	0.5	0.00000	-0.50000	0.54411	
	Thermal Parameters						
	Atom	U_{11}	U_{22}	U_{33}	U_{12}	U_{13}	U_{23}
	Ti	0.06152	0.06152	0.05854	0.00000	0.00000	0.00000
	O	0.03355	0.09120	0.06239	0.00000	0.00000	0.00000
750ºC	Anatase	TiO_2	Tetragonal	$I4_1/amd$ (no. 141)	a = 3.8037(20); c = 9.5976(20)	138.86(11)	3.821
	Atomic Coordinates						
	Atom	Position	Occupancy	x	y	z	
	Ti	4*b*	1	0.00000	0.00000	0.50000	
	O	8*e*	1	0.00000	0.00000	0.30222	
	Thermal Parameters						
	Atom	U_{11}	U_{22}	U_{33}	U_{12}	U_{13}	U_{23}
	Ti	0.12198	0.12198	0.08396	0.00000	0.00000	0.00000
	O	0.09874	0.05268	0.11900	0.00000	0.00000	0.00000
	Rutile	TiO_2	Tetragonal	$P4_2/mnm$ (no. 136)	a = 4.6241(20); c = 2.9830(20)	63.78(6)	4.159
	Atomic Coordinates						
	Atom	Position	Occupancy	x	y	z	
	Ti	2*a*	1	0.00000	0.00000	0.00000	
	O	4*g*	1	0.30408	-0.30408	0.00000	
	Thermal Parameters						
	Atom	U_{11}	U_{22}	U_{33}	U_{12}	U_{13}	U_{23}
	Ti	0.05963	0.05963	0.03823	0.00314	0.00000	0.00000
	O	0.05282	0.05282	0.01933	0.00272	0.00000	0.00000
950ºC	Rutile	TiO_2	Tetragonal	$P4_2/mnm$ (no. 136)	a = 4.6306(20); c = 2.9889(20)	64.09(6)	4.139
	Atomic Coordinates						
	Atom	Position	Occupancy	x	y	z	
	Ti	2*a*	1	0.00000	0.00000	0.00000	
	O	4*f*	1	0.30629	0.30629	0.00000	
	Thermal Parameters						
	Atom	U_{11}	U_{22}	U_{33}	U_{12}	U_{13}	U_{23}
	Ti	0.06993	0.06993	0.06042	-0.00093	0.00000	0.00000
	O	0.05305	0.05305	0.06999	-0.00511	0.00000	0.00000

Conclusions

A facile synthesis method for titania (TiO_2) microspheres was successfully developed. In the morphology of TiO_2-polycrystalline, there is a distribution of microspheres of approximately 0.5 to 1.0 mm. The XRD and FT-Raman results indicated that TiO_2-polycrystalline microspheres showed TiO_2 (B) phase. The FT-Raman and FT-IR spectra suggested that a large amount of H_2O and NO_3^- anion were located on the surface and in the layers of the TiO_2-polycrystalline microspheres. The HT-XRD results indicated that diffraction peaks of TiO_2-polycrystalline microspheres are indexed as TiO_2 (B) phase at temperatures measurement from 100 to 250 ºC and as anatase phase at temperature measurement from 300 to 650 ºC. However, mixed crystals of anatase and rutile were observed at temperatures measurement from 700 to

800 °C. Pure rutile phase has formed at temperatures measurement from 850 to 1000 °C. The results of microstructure analysis show that the anatase structure could be indexed to $I4_1/amd$ (no. 141) space group with tetragonal symmetry at temperatures measurement: 600 and 750 °C, while the rutile structure could be indexed to $P4_2/mnm$ (no. 136) space group with tetragonal symmetry at 750 and 950 °C.

Acknowledgments

The research was supported by a grant from DIPA BLU FMIPA UNY 2016. The authors are grateful to thank for the financial support obtained from the Faculty Mathematics and Natural Science, Yogyakarta State University, Indonesia. One of the authors acknowledges the support of Luc Brohan (researcher of CNRS-IMN), Nantes, France.

References

1. B. O'Regan and M. Grätzel, Nature 353 (1991) 737-740.
2. C. Dwivedi, V. Dutta, A.K. Chandiran, Md. K. Nazeeruddin, and M. Grätzel. Energy Proced. 33 (2013) 223-227.
3. J.-H. Yum, R. Humphry-Baker, S.M. Zakeeruddin, Md. K. Nazeeruddin, and M. Grätzel, Nano Today 5[2] (2010) 91-98.
4. T.K. Ghorai and N. Biswas, J. Mater. Res. Technol. 2[1] (2013) 10-17.
5. A. Ashkarran, M. Fakhari, H. Hamidinezhad, H. Haddadi, and M. R. Nourani, J. Mater. Res. Technol. 4[2] (2015) 126-132.
6. D. Mardare, N. Cornei, C. Mita, D. Florea, A. Stancu, V. Tiron, A. Manole, and C. Adomnitei, Ceramic Inter. 42 [6] (2016) 7353-7359.
7. W. Cai, H. Yang, and X. Guo, Procedia Engineering 94 (2014) 71-75.
8. H. Miao, X. Hu, J. Fan, C. Li, Q. Sun, Y. Hao, G. Zhang, J. Bai, and X. Hou, Appl. Surf. Sci. 358[A] (2015) 418-424.
9. J. Yu, X. Zhao, Q. Zhao, and G. Wang, Mater. Chem. Phys. 68[1-3] (2001) 253-259.
10. Y. Tsuge, J. Kim, Y. Sone, O. Kuwaki, and S. Shiratori, Thin Solid Films 516[9] (2008) 2463-2468.
11. X. Ding, Sh. Zhou, L. Wu, G. Gu, and J. Yang, Surf. Coat. Tech. 205[7] (2010) 2554-2561.
12. X. Zhang, M. Li, X. He, R. Hang, X. Huang, Y. Wang, X. Yao, and B. Tang, Appl. Surf. Sci. 372 (2016) 139-144.
13. Y. Chen, Y. Deng, Y. Pu, B. Tang, Y. Su, and J. Tang, Mater. Sci. Eng. C65 (2016) 27-32.
14. T.E. Weirich, M. Winterer, S. Seifried, H. Hahn, and H. Fuess, Ultramicroscopy 81[3-4] (2000) 263-270.
15. C.J. Howard, Z.M. Sabine, and F. Dickson, Acta Crystal. B47 (1991) 462-468.
16. R.J. Swope, J.R. Smyth, and A.C. Larson, Am. Mineral. 80 (1995) 448-453.
17. W. Luo, S.F. Yang, Z.C. Wang, Y. Wang, R. Ahuja, B. Johanssonb, J. Liu, and G.T. Zou, Solid State Commun. 133 (2005) 49-53.
18. R. Marchan, L. Brohan, and M. Tournoux, Mat. Res. Bull. 15 (1980) 1129-1133.
19. M. Latroche, L. Brohan, R. Marchand, and M. Tournoux, J. Solid State Chem. 81 (1989) 78-82.
20. J. Akimoto, Y. Gotoh, Y. Osawa, N. Nonose, T. Kumagai, K. Aoki, and H. Takei, J. Solid State Chem. 113 (1994) 27-36.
21. I. E. Grey, C. Li, I.C. Madsen, and G. Braunshausen, Mat. Res. Bull. 23[5] (1988) 743-753.
22. M.Y. Kuo, C.L. Chen, C.Y. Hua, H.C. Yang, and P. Shen, J. Phys. Chem. B. 109 (2005) 8693-8700.
23. N.A. Dubrovinskaia, L.S. Dubrovinsky, R. Ahuja, V.B. Prokopenko, V. Dmitriev, H.P. Weber, J.M. Osorio-Guillen, and B. Johansson, Phys. Rev. Lett. 87[27] (2001) 275501-275503.
24. M. Mattesini, J.S. De Almeida, L. Dubrovinsky, N. Dubrovinskaia, B. Johansson, and R. Ahuja, Phys. Rev. B70 (2004) 212101.
25. G. Cabello, R.A. Davoglio, and E.C. Pereira, J. Electroanal. Chem. 794[1] 36-42.
26. A. Selloni, Nature Material 7 (2008) 613-615.
27. Z. Wei, E. Kowalska, K. Wang, C. Colbeau-Justin, and B. Ohtani, Catal. Today 280[1] (2017) 29-36.
28. Y. Gao, H. Wang, J. Wu, R. Zhao, Y. Lu, and B. Xin, Appl. Surf. Sci. 294[1] (2014) 36-41.
29. J. Zhang, B. Wu, L. Huang, P. Liu, X. Wang, Z. Lu, G. Xu, E. Zhang, H. Wang, Z. Kong, J. Xi, and Z. Ji, J. Alloy. Comp. 661 (2016) 441-447.
30. Q. Sheng, S. Yuan, J. Zhang, and F. Chen, Micropor. Mesopor. Mat. 87[3] (2006) 177-184.
31. U. Černigoj, U.L. Štangar, P. Trebše, U.O. Krašovec, and S. Gross, Thin Solid Films 495[1-2] (2006) 327-332.
32. B. Sarkar, N. Singhal, R. Goyal, A. Bordoloi, L.N. S. Konathala, U. Kumar, and R. Bal, Catal. Commun. 74 (2016) 43-48.
33. S.B. Khan, M. Hou, S. Shuang, and Z. Zhang, Appl. Surf. Sci. 400 (2017) 184-193.
34. K.K. Tehare, S.S. Bhande, S.U. Mutkule, F.J. Stadler, J.-P. Ao, R.S. Mane, and X. Liu, J. Alloy. Comp. 704 (2017) 187-192.
35. W.I.F. David, K. Shankland, L.B. McCusker, and Ch. Baerlocher, "Structure Determination from Powder Diffraction Data" (IUCr Monographs on Crystallography 13, Oxford University Press, 2002).
36. G. Will, "Powder Diffraction: The Rietveld Method and the Two Stage Method to Determine and Refine Crystal Structures from Powder Diffraction Data" (Springer, 2005).
37. T. Roisnel and J. Ridriguez-Carvajal, "WinPLOTR a Graphic Tool for Powder Diffraction" (Rennes: CNRS-Lab. de Chimie du Solide et Inorganique Moléculaire Université de Rennes, 2001).
38. P. McArdle, K. Gilligan, D. Cunningham, R. Dark, and J. Mahon, "Oscail-X version 2.1.6" (NUI Galway: Crystallography Center, School of Chemistry, 2008).
39. M. Ben Yahia, F. Lemoigno, T. Beuvier, J.S. Filhol, M. Richard-Plouet, L. Brohan, and M.L. Doublet, J. Chem. Phys. 130 (2009) 204501(1-11).
40. H. Sutrisno, J. Sains Dasar 1[1] (2012) 18-32.
41. T. Beuvier, M. Richard-Plouet, and L. Brohan, J. Phys. Chem. C 113 (2009) 13703-13706.
42. N.B. Colthup, L.H. Daly, and S.E. Wiberly, "Introduction to Infrared and Raman Spectroscopy" (Academic Press, 1990).
43. B. Kolesov, Am. Mineral. 91 (2006) 1355-1362.
44. M. Malferrari, G. Venturoli, F. Francia, and A. Mezzetti. Spectroscopy: An International Journal. 27[5-6] (2012) 337-342.
45. B. Stuart, "Infra Red Spectroscoy: Fundamentals and Applications" (John Wiley and Sons Ltd., 2004) p. 82, p.174.